Reactivation Potential of Intraplate Faults in the Western Quebec Seismic Zone, Eastern Canada

Jeremy Rimando[1], Alexander Peace[1]

[1]School of Earth, Environment and Society, McMaster University, Hamilton, Ontario, Canada

*Corresponding author: Jeremy Rimando
Email: rimandoj@mcmaster.ca

Abstract

The intraplate western Quebec seismic Zone (WQSZ) in eastern Canada experiences moderate seismicity that mainly results from reactivation of inherited structures under the present-day, NE-striking regional stress field and, possibly to a minor extent, through stress perturbations in response to glacio-isostatic adjustments. This work comprises the first numerical stress simulation-based study that predicts the preferred spatial distribution, trends, and sense of slip of contemporary fault reactivation, which may have implications for possible fault segmentation patterns in the WQSZ. We show that NNW- to NW-striking faults, mostly in the western sector of the WQSZ, exhibit the highest slip tendency values. Spatial patterns of slip tendency and kinematics of reactivation are consistent with the observed seismicity. In an area where Quaternary-active faults have yet to be systematically identified, we have narrowed down areas to focus on for more detailed, future neotectonic investigations that could provide sound foundation for seismic hazard assessments.

1. Introduction

The western Quebec seismic zone (WQSZ; **Fig. 1**) in eastern Canada is an extensive, intraplate continental region characterized by spatial clustering of weak to moderate recent seismicity (**Fig. 2**) which likely results mainly from the reactivation under the present-day tectonic stress field of inherited structures such as late Precambrian to early Paleozoic Iapetan rifts and aulacogens, as well as Precambrian suture zones and plate boundaries (**Culotta et al, 1990; Kumarapelli, 1978; Rimando, 1994; Rimando and Benn, 2006**). Major tectonic features in the area include grabens and half-grabens that belong to the Saint Lawrence Rift system, such as the Ottawa-Bonnechere and Timiskaming grabens (**Fig. 1A**), that are composed primarily of NW- and NE-striking, steeply dipping valley-forming faults (**Fig. 1B; Kay, 1942; Lamontagne et al., 2020, and references therein; Lovell & Caine, 1970**). These affect the Precambrian basement of the Canadian Shield and the Paleozoic sedimentary sequences of the Saint Lawrence-Ottawa Platform, and are associated with most of the topographic relief in this region (**Fig. 1**). The current tectonic stress field in eastern North America is well constrained and, as with most other continental plate interiors, is broadly uniform (**Mazzotti and Townend, 2010**). Borehole breakout measurements and inversions of earthquake focal mechanisms consistently indicate a maximum horizontal compressive stress axis (S_H) that is oriented NE-SW (**Mazzotti and Townend, 2010; Reiter et al., 2014, Snee and Zoback, 2020**), which is attributed to spreading along the Mid-Atlantic Ridge (**Richardson, 1992**).

Remarkably, despite the seismicity, only a handful of active faults with surface expression in the WQSZ have been identified and mapped to date. In the WQSZ, the Timiskaming Graben (**Fig. 1B**), for instance, has been identified as active from seismotectonic analysis and from evidence of coseismic ground deformation following the moment magnitude (M_W) 6.1 Timiskaming earthquake (**Fig 2A&B; Bent, 1996; Doughty et al., 2012**). Conversely, some recent earthquakes, such as the 2010 M_W 5.2 Val des Bois (**Atkinson & Assatourians, 2010; Ma & Motazedian, 2012**) and 2013 M_W 4.7 Ladysmith earthquakes (**Ma & Audet, 2014**), are associated with well-defined source mechanisms and locations, but have yet to be associated with their causative faults. Eastern Canada, including the WQSZ, is currently lacking a comprehensive, reliable assessment of seismic hazards, due to the scarcity of detailed earthquake source models, typically from a combination of seismic, geologic, and/or geodetic data (**Morell et al., 2020**). Further complicating our poor understanding of fault reactivation and seismicity in eastern Canada is the fact that most evidence of initiation of fault activity under the current stress regime typically postdates glaciation (**Adams, 1989**). There is a debate over whether recent faulting occurs as a result of tectonic stress or glacio-isostatic adjustment, or both (**e.g., Adams, 1989; Brooks and Adams, 2020; Wallach et al., 1995**). Despite the surficial nature and exposure of some pop-up structures and offset boreholes within quarries in Ontario and Quebec, a tectonic origin is the preferred interpretation for most of these features due to the compatibility of their orientations and kinematics with the current regional stress field in eastern North America (**Wallach and Chagnon, 1990; Wallach et al, 1993; Wallach et al., 1995**). Besides, detailed studies of the state of stress in eastern Canada (**Mazzotti and Townend, 2010**) indicate that magnitudes of long-wavelength stress perturbations such as postglacial rebound stresses are an order of magnitude lower, hence minor in comparison to mid-crustal stresses. It is possible, however, for postglacial rebound stress to cause high enough stress perturbations if these are concentrated on faults with an unusually low coefficient of friction ($\mu \sim 0.1$).

Knowledge of the nature, distribution, and extent of seismogenic structures in Eastern Canada, including their potential for causing large magnitude earthquakes is of paramount socio-economic importance (e.g., **Morell et al., 2020**). A major earthquake in eastern Canada could trigger a chain of events in the insurance industry and have far-reaching economic consequences (**Le Pan, 2016**). However, there is currently no map of the active structures in the WQSZ, a region which hosts major population centers, including Ottawa—the seat of Canada’s national government. As in most intraplate settings, there is a rarity of well-preserved recent fault/fold scarps in the WQSZ (**McCalpin, 2009**), probably as a result of long recurrence intervals on slow-moving faults (**Stein, 2007**), and due to glacial peneplanation (**Dyke et al., 2002**). Similarly, the short temporal coverage of instrumental seismicity records is not enough to create an inventory of detailed earthquake source models and to determine earthquake recurrence intervals in intraplate regions. However, we know from worldwide examples that large earthquakes are far more common than previously thought in “stable continental regions” (**Calais et al., 2016; Rimando et al., 2021**). In eastern North America, instrumental, historical, and paleoseismic records show that the region has been shaken by devastating earthquakes, such as the 1929 M_S 7.2 Grand Banks and the 1811-1812 M_W 7.2-8.2 New Madrid earthquakes) (**Bent et al., 1995; Hasegawa & Kanamori, 1987; Tuttle, et al., 2002**).

In the absence of a map of active faults, a good first step is to determine the potential of pre-existing faults to be reactivated under the current stress field. A good correlation between relatively high slip tendency and evidence of Quaternary activity has been shown in different tectonic settings with wide-ranging levels of seismic activity (e.g., **Worum et al., 2004; Yukutake et al., 2015**). While previous studies have described conceptually the likely orientation and kinematics of fault reactivation under the current stress field (**Daneshfar and Benn, 2002; Rimando, 1994; Rimando and Benn, 2005)**, no work has characterized in detail the slip tendency and expected slip directions of specific faults in the WQSZ. This work presents the first study which uses 3D numerical stress simulations to explore the preferred spatial distribution and trends, and predicted sense of slip of reactivated pre-existing structures in the WQSZ under the current tectonic stress field. We show how fault reactivation potential studies can be useful for identifying key areas or fault populations to focus on for more detailed seismic hazard assessment.

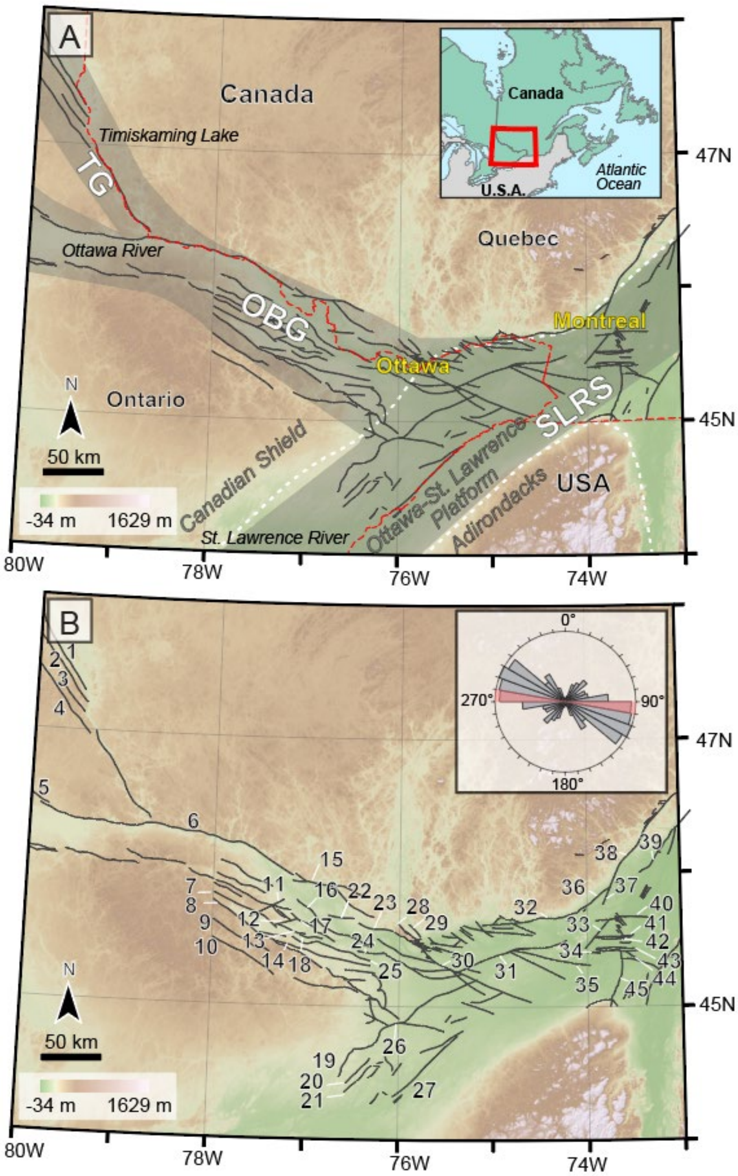

Figure 1. A) Major tectonic features of the Western Quebec seismic zone (WQSZ). TG–Timiskaming Graben. OBG–Ottawa-Bonnechere Graben. SLRS–Saint Lawrence Rift System. White dashed line indicates the boundaries of geological provinces: Canadian Shield, Ottawa-St. Lawrence Platform, and the Adirondacks. Red dashed line indicates political boundaries. Inset map shows the location of the WQSZ in eastern North America. **B)** Faults in the WQSZ. The orientations of faults are summarized by a rose diagram which has 18 bins (10° intervals). 1–Timiskaming, 2–Cross Lake, 3–Montreal River, 4–Latchford, 5–Crystal Falls, 6–Mattawa River, 7–Deacon, 8–St. Patrick, 9–Hopefield, 10–Madawska, 11–Gardez Pieds, 12–Cochran, 13–Eganville, 14–Shamrock, 15–Coulonge, 16–Muskrat, 17–Dore, 18–Douglas, 19–Canoe-Dessert Lake, 20–Sydenham Lake, 21–Loughborough Lake, 22–Rocher Fendu, 23–Eardley, 24–Hazeldean, 25–Packenham, 26–Rideau Lakes, 27–St. Lawrence River, 28–Meech Lake, 29–Gatineau River, 30–Gloucester, 31–Russel Rigaud, 32–Lachute, 33–Milles Iles, 34–Sainte-Anne-de-Bellevue, 35-Sainte-Justine, 36–New-Glasgow, 37–Sainte-Julienne, 38–Saint-Maurice, 39–Saint-Cuthbert, 40–Bas-de-Sainte-Rose, 41–Rapide-du-Cheval Blanc, 42–Ile Bizard, 43–Dorval, 44–Saint-Regis, 45–Havelock. The topography is derived from a 30-m-resolution Advanced Spaceborne Thermal Emission and Reflection Radiometer (ASTER) global digital elevation models (GDEM) (https:// asterweb.jpl.nasa.gov/gdem.asp).

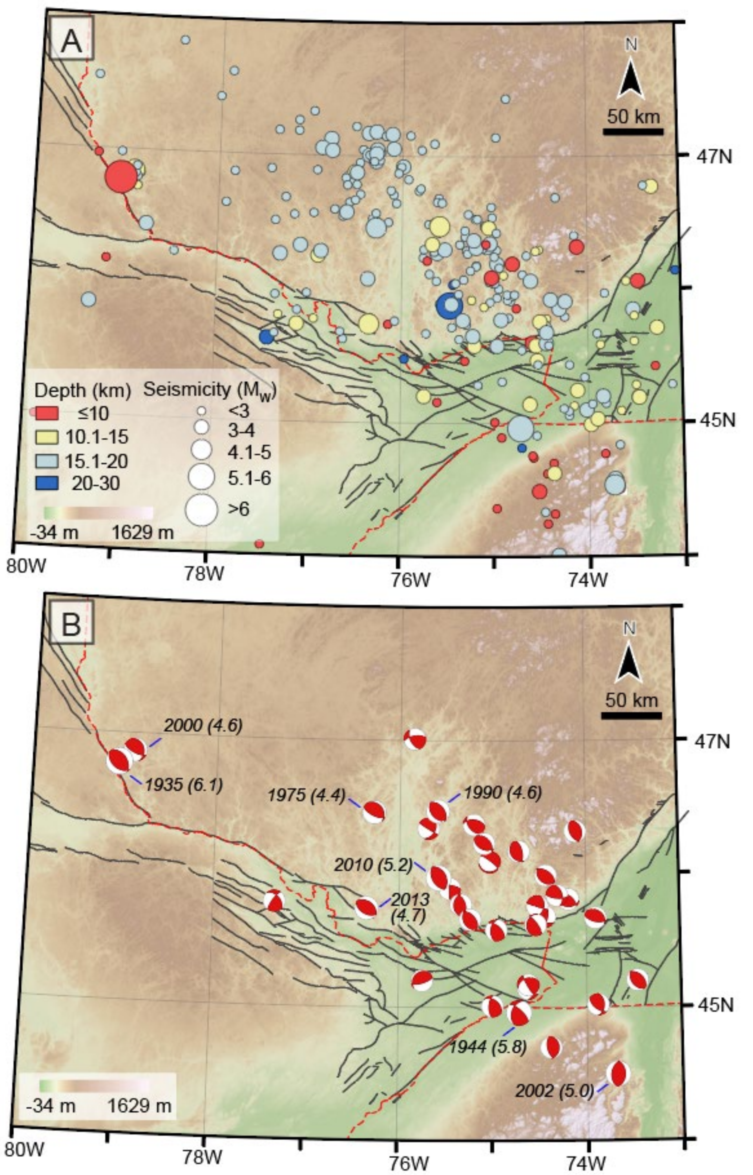

Figure 2. Seismicity in the WQSZ. **A)** Earthquake epicentral plots color-coded according to depth and scaled to magnitude. **B)** Earthquake focal mechanisms with labels of year and magnitude of notable events. Well-localized seismicity is from Adams et al. (1988, 1989), Bent et al. (1996, 2002, 2003), Du et al. (2003), Horner et al. (1978), Ma & Eaton (2007), Seeber et al. (2002), Wahlstrom et al. (1987), and the earthquake bulletins of both the Natural Resources Canada (NRCan; https://earthquakescanada.nrcan.gc.ca/index-en.php) and the United States Geological Survey (USGS; https://www.usgs.gov/natural-hazards/earthquake-hazards/earthquakes).

2. Data and Methods

Slip Tendency (**Morris et al., 1996**) is the ratio of the shear stress to normal stress on a fault surface, which is expressed as the following equation:

$$T_s = \tau/\sigma_n, \qquad (\mathbf{1})$$

where T_S is the slip tendency, τ is the shear stress, and σ_n is the normal stress.

Slip tendency analysis has been used in different tectonic settings worldwide to characterize the relative likelihood of populations of faults to slip under current or past stress fields (e.g., **Morris et al., 1996; Peace et al., 2018; Worum et al., 2004**). Faults that are likely to slip are those with a higher ratio of shear stress to normal stress. Faults subject to a certain stress field are characterized as “optimally oriented” if the set of strike and dips yield high slip tendency values.

It should be noted, however, that we make implicit assumptions in using this technique, which introduce some limitations on how closely our model represents reality. Following the Wallace-Bott hypothesis (**Wallace, 1951; Bott, 1959**) wherein slip on faults is expected to occur along the direction of the maximum resolved shear stress, this method assumes simple planar faults and a relatively uniform stress field, and it neglects fault interaction, fault block rotation, and internal deformation. Despite these caveats, it has been shown through numerical studies to be a good first order approximation (**Dupin et al., 1993; Pollard et al., 1993**), as the deviation between actual and theoretical slip directions are on average less than 10°. A strong match between modelled slip tendencies and directions and natural reactivated fault plane orientations and slip directions from global geological and seismological datasets lends support to the use of slip tendency analysis as a useful prediction tool (**Collettini and Trippetta, 2007; Lisle and Srivastava, 2004**).

We modelled the reactivation potential of faults in the WQSZ using the 'Slip Tendency' function in the 'Stress Analysis' module of the software Move™ by Petroleum Experts Limited (https://www.petex.com/), and determined the predicted sense of fault slip using the 'Slicken 1.0' software (**Xu et al., 2017**). In both software, the stress tensor and fault plane orientations were the required inputs.

We primarily used the average (45°) maximum horizontal compressive stress axis (S_H) azimuth value but also ran simulations using the extreme values (28° and 73°) determined for the Montreal and Gatineau zones by **Mazzotti and Townend (2010)**. These were based both on Bayesian inversion of earthquake focal mechanisms and calculation of the weighted averages (weights based on quality) of borehole breakout stress measurements within 250 km of the area of interest. The orientations of S_H measured from both sources were consistent and roughly parallel. Focal mechanism inversions revealed a nearly vertical σ_3 and nearly horizontal σ_1 and σ_2, defining a reverse faulting stress regime, which is consistent with findings of previous crustal stress orientation studies (**Heidbach et al., 2010; Reiter et al., 2014, Snee and Zoback, 2020**). Knowing that σ_1 is horizontal enabled us to use the S_H from borehole measurements as an approximation for σ_1.

We estimated regional stress magnitudes by assuming a critically stressed crust model (**Townend and Zoback, 2000; Zoback and Zoback, 2002**), in which differential stress values are at a level such that optimally-oriented Andersonian faults are on the verge of slipping. In a reverse-faulting stress regime the principal stresses can be computed using the following equations:

$$\sigma_1 - \sigma_3 = \rho g z(\lambda - 1)(1 - F)\,, \qquad (\mathbf{2})$$

$$\sigma_3 = (1 - \lambda)\rho g z\,, \qquad (\mathbf{3})$$

$$R = \frac{\sigma_1 - \sigma_2}{\sigma_1 - \sigma_3}\,, \qquad (\mathbf{4})$$

$$F = \left(\sqrt{\mu^2 + 1} + \mu\right)^2, \qquad (\mathbf{5})$$

where σ_1 is the maximum effective horizontal stress, σ_2 is the minimum effective horizontal stress, σ_3 is the effective vertical stress, λ is the pore-fluid factor (pore fluid pressure, P_f divided by the σ_3), ρ is average crustal density (2700 g/m^3), g is gravitational acceleration (9.8 m/s^2), z is depth (in meters), R is the principal stress difference ratio (typically 0.6 in intraplate continental regions), F is the frictional parameter, and μ is the coefficient of friction.

We calculated the stress magnitudes at a mid-seismogenic zone depth of 10 km. Our choice of coefficient of friction (μ) and pore fluid factor (λ) values considers the fact that the maximum possible differential stress (σ_1- σ_3) values at mid-crustal depths in this region are unlikely to exceed 200 megapascals (MPa), which is based on previous modelling studies and extrapolation of in-situ field measurements at shallower depths in Canada and in intraplate settings in general (e.g., **Hasegawa et al., 1985; Lamontagne and Ranalli, 1996, and references therein**). This condition of relatively low differential stress necessitates the μ and λ values to be lower and higher, respectively, than the values that are commonly assumed (e.g., **Byerlee, 1978; Townend and Zoback, 2000**). For the purposes of this study, we used a σ_1- σ_3 value close to the 200 MPa upper limit. We adapted a μ of 0.5 and a λ of 0.6, which are intermediate to the values previously determined from modelling of the conditions for slip of earthquakes in southeastern Canada (**Zoback, 1992**). A low coefficient of friction is at shallow depths likely results from the presence of thick phyllosilicate-rich fault gouges (**e.g., den Hartog et al., 2000**) and in the mid-crust through the presence of a dense network of fractures and faults (**Ito and Zoback, 2000**). The upward migration of mantle-derived mixed H_2O-CO_2 fluids is a proposed source of high pore fluid pressure that enables the reactivation of high-angle faults in eastern Canada (Sibson, 1989). Hence, we applied the following stress tensors in our analyses: σ_1 = N28°E-N73°E= 277.09 MPa, σ_2 = N118°E-N163°E = 174.34 MPa, and σ_3 = vertical = 105.84 MPa.

With the exception of a few faults, information on the deeper structure of most faults is lacking in the WQSZ. Where available, information on the geometry of faults from subsurface imaging techniques is confined to depths of less than a 100 m at best (e.g.,

Doughty et al., 2012). However, most papers, reports, and geological cross-sections on the area indicate steep fault dips with an average of around 60° (**e.g., Lovell & Caine,1970; Rocher & Tremblay, 2001; Rimando, 1994**). We therefore assumed a dip of 60° to build 3D fault surface models. The 3D models were built by projecting surfaces from shapefiles of the Geological Survey of Canada's latest WQSZ faults map (**Lamontagne et al., 2020**). We also ran simulations over a range of fault dips (at 15° increments) to test the effect of underestimating or overestimating the actual fault dip on the calculated slip potential and sense of slip of faults.

3. Results

Our slip tendency analysis reveals that by applying a stress field oriented σ_1 = N28°E-N73°E = 277.09 MPa, σ_2 = N118°E-N163°E = 174.34 MPa, and σ_3 = vertical = 105.84 MPa, and assuming a dip of 60 degrees on faults in the WQSZ, that NNW- to NW-striking faults, mostly on the western sector of the WQSZ tend to have relatively higher slip tendencies (compared to the more NE-striking faults in the eastern sector), and are therefore, considered optimally oriented to be reactivated (**Fig. 3A**). Faults are predicted to slip mostly either as pure reverse faults or as oblique reverse faults (**Fig. 3B**). The magnitude and spatial distribution of the slip tendency varies, albeit insignificantly, over the range of the assumed possible orientations of σ_1 (i.e., 28°, 45°, 73°). For instance, the average slip tendency values of NW- striking and NE- striking faults (for 60° dip) vary on average by ~5% and ~10% of each other, respectively (**Fig. 3A** and **Supplementary Table S1**). On the other hand, the preferred kinematics of slip has a more noticeable spatial variation. Faults that are oriented perpendicularly to σ_1 are expected to be reactivated with a pure reverse slip. Consequently, the distribution of pure reverse faults appears to rotate clockwise as the σ_1 azimuth is increased, and coincidentally, decreases in abundance due to the decreasing number of faults oriented at a high angle to the σ_1 in the WQSZ (**Fig. 3B**). While the magnitudes of slip tendency appear to vary as a function of the assumed fault dip, the western sector of the WQSZ exhibits generally relatively higher slip tendencies, with average values of NW-striking faults being 20% higher than

NE-striking faults for σ_1 = 45° (**Fig. 4; Supplementary Table S1**). The predicted slip in the 15° to 60° dip scenarios all exhibit either pure reverse or oblique reverse faulting. It is notable that in the 75° dip scenario, there tends to be significantly more faults with a dominant strike-slip component, and in the 90° dip scenario, faults are expected to be reactivated almost entirely as pure strike-slip faults (**Fig. 5**). Additionally, for faults dipping 75° and 90° with σ_1 = 28° & 45°, NE-striking faults tend to have slightly higher average slip tendency values than NW-striking faults, possibly due to these faults being optimally oriented to be reactivated with a dominant strike-slip component (**Supplementary Figures S1-4; Supplementary Table S1**). It is worth noting that, with exception to the 30° dip scenario (which seems to be the optimal dip for fault reactivation in the WQSZ), slip tendency values decrease as the assumed fault dip increases (**Fig. 4**). Most of these observations on the variations of slip tendency and expected slip direction as a function of dip and as a function of σ_1 orientation, apply as well to other σ_1 orientation scenarios (σ_1 = 28° and σ_1 = 73°) and to the different dip scenarios (15°, 30°, 45°, 75°, and 90°), respectively (**Supplementary Figures SS1-4**).

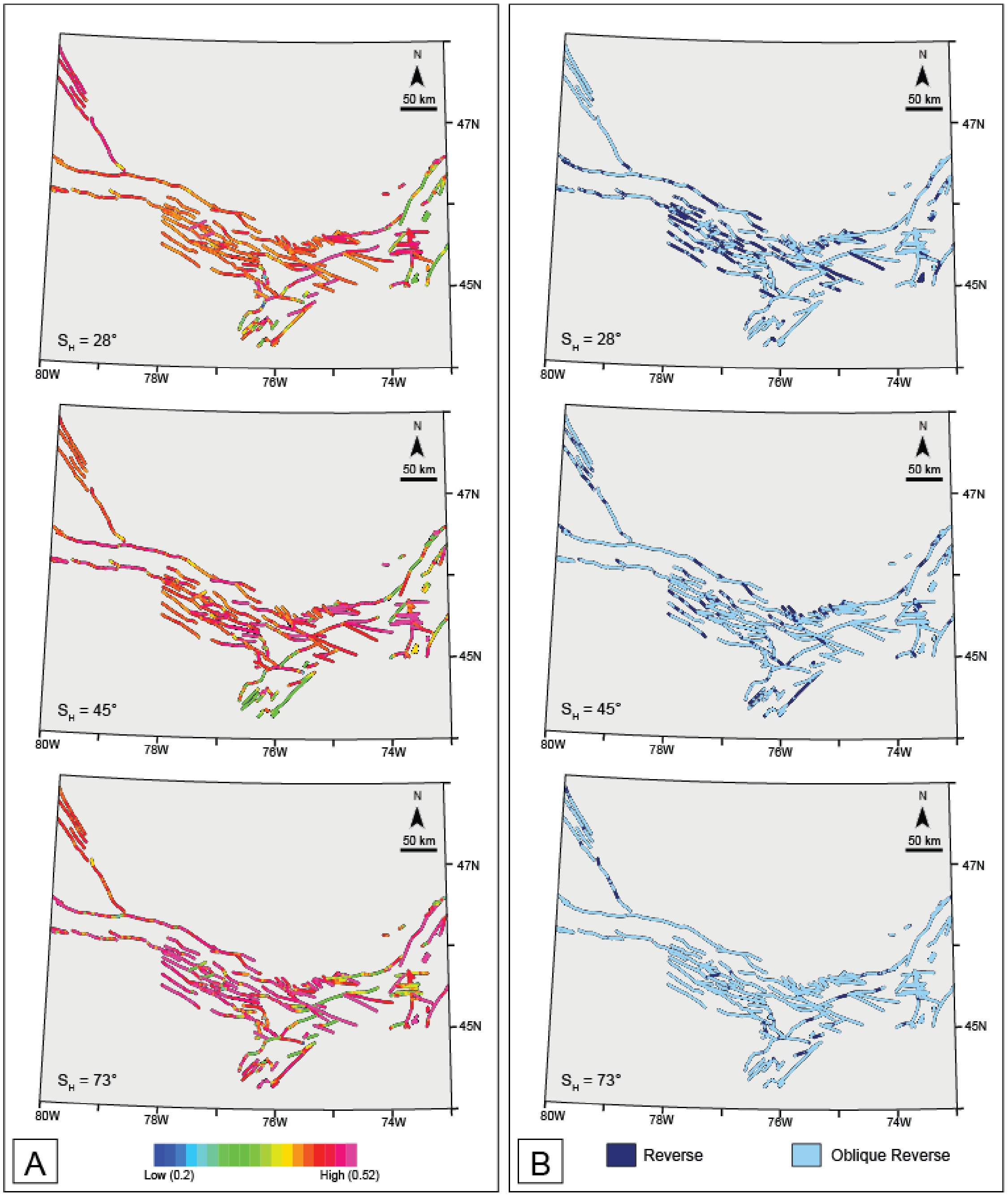

280

281 **Figure 3. A)** Slip tendency maps and **B)** Predicted slip kinematics of faults dipping 60° with S_H azimuth

282 values of 28°, 45°, 73°.

283

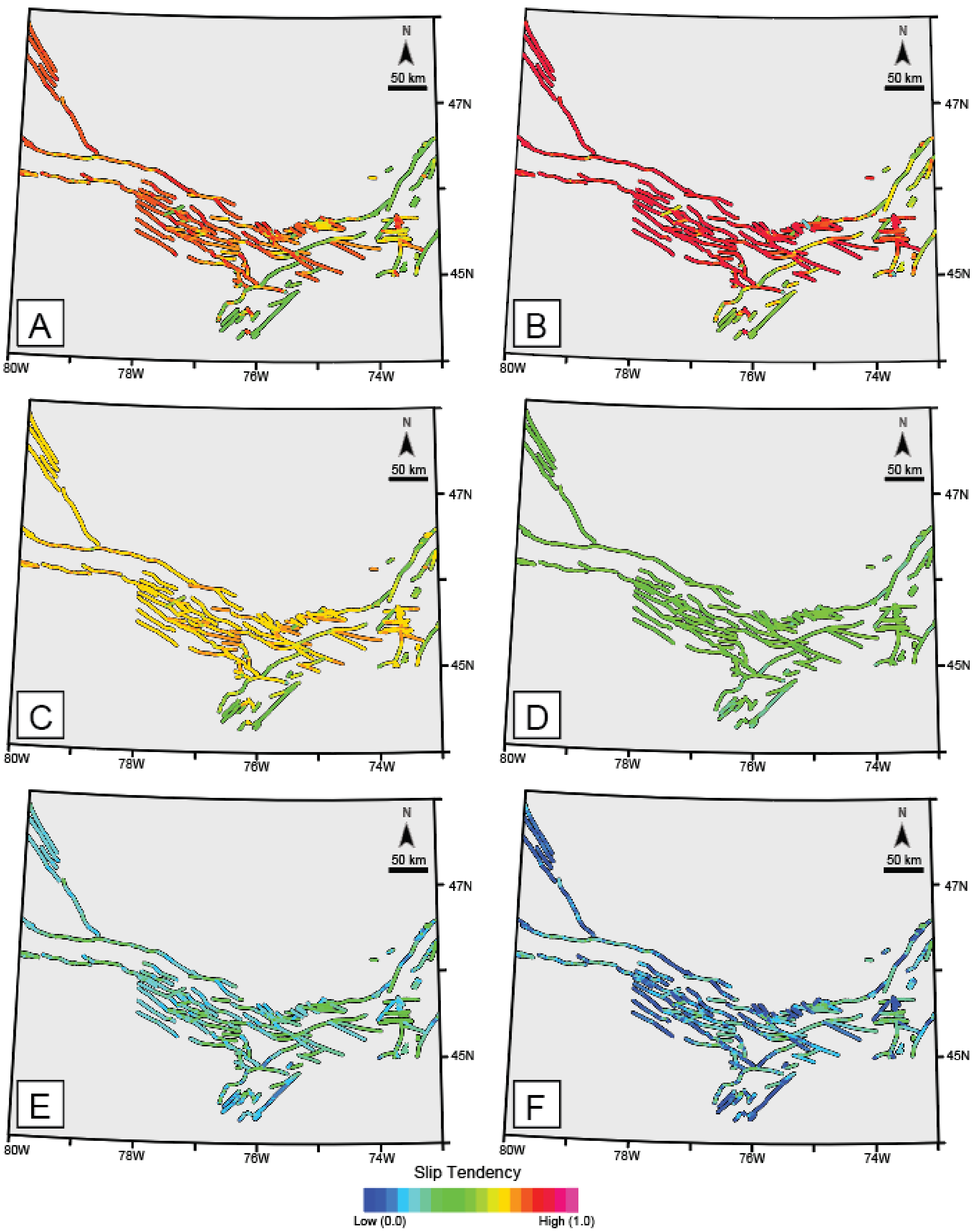

Figure 4. Slip tendency maps for different fault dip scenarios (with an S_H azimuth of 45°). **A)** 15°, **B)** 30°, **C)** 45°, **D)** 60°, **E)** 75°, and **F)** 90°.

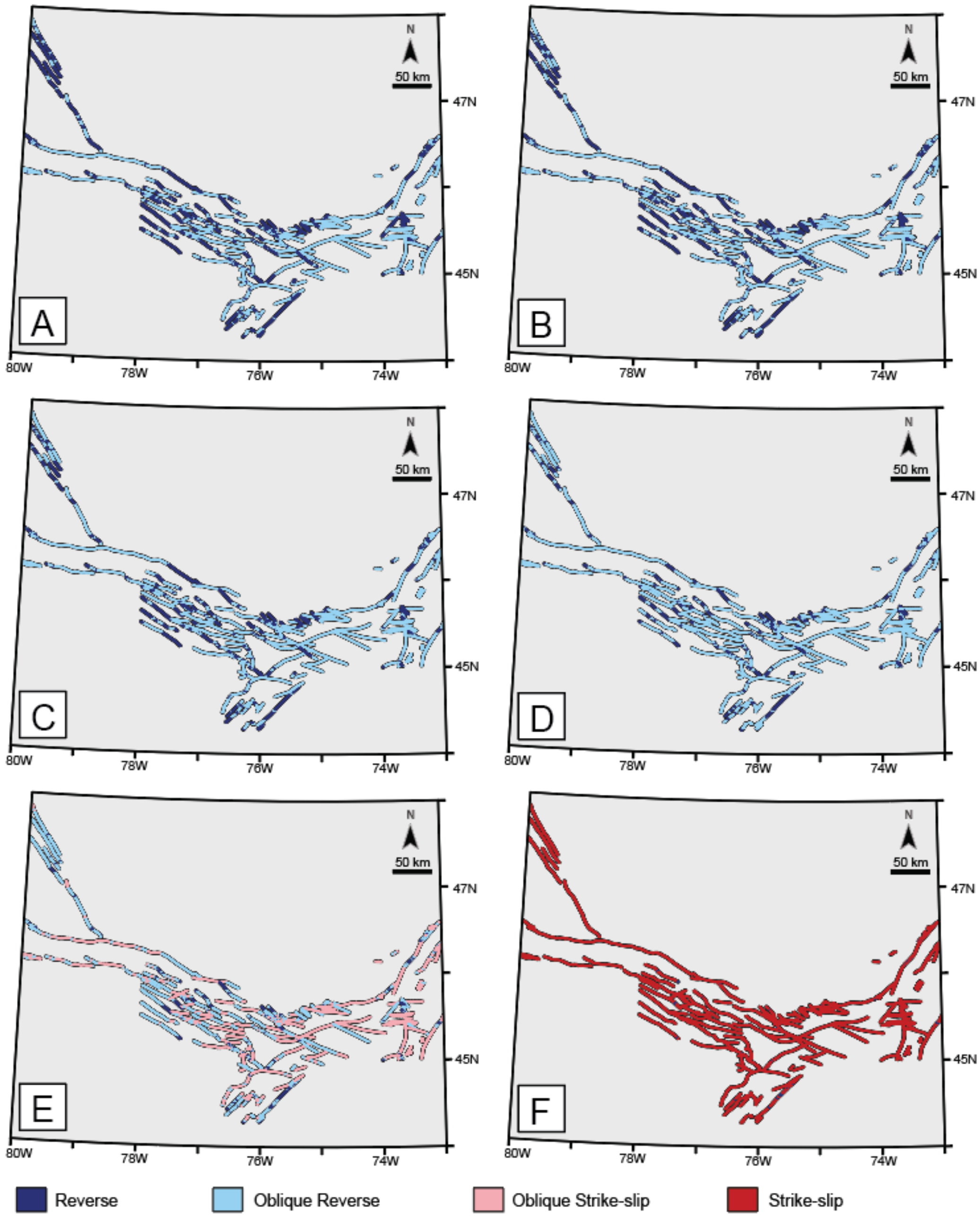

Figure 5. Predicted slip kinematics for different fault dip scenarios (with an S_H azimuth of 45°). **A)** 15°, **B)** 30°, **C)** 45°, **D)** 60°, **E)** 75°, and **F)** 90°.

4. Discussion and Conclusions

Our results show that the NNW- to NW-striking faults that are found mostly in the western sector of the WQSZ consistently exhibit relatively higher slip tendency values. However, although we considered the effect of adapting different dip values, we modelled dips uniformly across the WQSZ during each simulation. In reality, however, it is unlikely the case that the dips of all the faults in the WQSZ are uniform. Nonetheless, unless the faults in the west sector are all dipping vertically or nearly vertically, and assuming that the Wallace-Bott hypothesis applies and pore fluid pressure conditions and fault frictional properties vary insignificantly throughout the WQSZ, then the slip tendency values of the faults in western sector are expected to be higher in the western sector for most conceivable variable-dip scenarios.

There is also a good correspondence between the modelled kinematics of fault reactivation (i.e., predominantly reverse and oblique reverse) (**Fig. 3B & 5**) under the assumed range of stress tensors and the actual kinematics of recent natural seismicity as indicated by earthquake focal mechanisms (**Fig. 2B**). Additionally, in upstate New York and southeastern Ontario, previous work has demonstrated that recent natural seismicity is spatially associated dominantly with NW-striking population of faults (**Rimando, 1994; Daneshfar and Benn, 2002**). Therefore, there seems to be multiple lines of evidence that give credence to the results of our modelling.

In reality however, the assumptions of the Wallace-Bott hypothesis are rarely entirely met (**Lisle, 2013**), which could feasibly cause deviations between our modelling results and the actual fault activity and kinematics. The results of this study, nonetheless, should provide a first order approximation of the distribution fault activity in the WQSZ. It can be argued, however, that the orientation of stress is fairly homogenous in the region, and the effects of fault block rotations and fault interactions are unlikely to significantly affect our results given the scale of our study area and the resolution of our modelling. Afterall, it is possible that the objections to the assumptions of the Wallace-Bott hypothesis may apply only at a relatively local scale (**Lisle, 2013**).

Future numerical stress simulations would benefit from more detailed 3D fault geometry models. For instance, some faults in the region have been shown to exhibit flat-ramp-flat and listric fault geometries (**Busch et al., 1996; Rimando and Benn, 2006**), which could possibly result in more complex along-strike and down-dip patterns of slip tendency and slip directions. Future studies should consider improving 3D fault models by integrating data from geophysical subsurface imaging, natural and trenching exposures, and seismicity. Having such data will not only reduce the uncertainty in our modelling, but will also help address concerns regarding the validity of the approach used in this study.

Our findings on the range of conditions in which faults in the WQSZ may experience reactivation has implications for the assessment of seismic hazards in the area. For instance, possible structural segmentation of individual faults can be inferred where abrupt change in fault slip tendency values is exhibited in our slip tendency and slip directions type maps (**e.g., Fig 3**). The length of segments can be used to estimate possible earthquake magnitudes based on scaling relationships between moment magnitude (M_W) and fault length (**Wells and Coppersmith, 1994**). As such, more appropriate and realistic M_W estimates can be made with the available slip type constraints. Additionally, the areal extent over which long-period ground motions occur has also been demonstrated to vary as a function of the style of faulting (**Aagaard et al., 2004**), and our results place constraints on the style of faulting.

Lastly, while this work brings us one step forward in our efforts to assess the activity of faults in the WQSZ, caution should be taken with mistaking slip tendency as the risk for fault rupture (**Yukutake et al., 2015**). The probability of an earthquake occurring on certain faults is a topic which is best tackled by more appropriate neotectonic analyses. Indeed, knowledge of which faults are more likely to be reactivated in the WQSZ can help earthquake geologists narrow down which faults/regions to prioritize and focus on for more detailed active fault mapping and paleoseismic studies for earthquake magnitude and recurrence interval estimation.

Acknowledgements

Dr. Jeremy Rimando's postdoctoral fellowship at McMaster University was gratefully funded in part by the Keith Macdonald structural geology fund which made this work possible. We would like to acknowledge Mr. Alan Vaughan and Dr. Cathal Reilly of Petroleum Experts Ltd for their assistance with the MOVE™ Software. We would also like to thank Dr. Mark Zoback (Stanford University), Dr. Elena Konstaninovskaya (University of Alberta), and Dr. Maurice Lamontagne (Geological Survey of Canada) for the very helpful discussions about the assumptions behind the parameters used for modelling slip tendency in eastern Canada.

Data Availability Statement

Data in this study were uploaded into the open-access Zenodo repository: Western Quebec Seismic Zone modelled slip tendencies and slip directions. http://doi.org/10.5281/zenodo.4698531 (Rimando and Peace, 2021).

References

Aagaard, B. T., Hall, J. F., & Heaton, T. H. (2004). Effects of fault dip and slip rake angles on near-source ground motions: Why rupture directivity was minimal in the 1999 Chi-Chi, Taiwan, earthquake. Bulletin of the Seismological Society of America, 94(1), 155-170. https://doi.org/10.1785/0120030053

Adams, J., Sharp, J., & Stagg, M.C. (1988). New focal mechanisms for southeastern Canadian earthquakes, Geological Survey of Canada Open File Report 1992, 109p. https://doi.org/10.4095/130428

Adams, J. (1989). Postglacial faulting in eastern Canada: nature, origin and seismic hazard implications. Tectonophysics, 163(3-4), 323-331. https://doi.org/10.1016/0040-1951(89)90267-9

Adams, J., Vonk, A., Pittman, D., & Vatcher, H. (1989). New focal mechanisms for southeastern Canadian earthquakes - Volume II, Geological Survey of Canada Open File Report 1995, 97 p. https://doi.org/10.4095/130594

Atkinson, G. M., & Assatourians, K. (2010). Attenuation and source characteristics of the 23 June 2010 M 5.0 Val-des-Bois, Quebec, earthquake. Seismological Research Letters, 81(5), 849-860. https://doi.org/10.1785/gssrl.81.5.849

Bent, A. L. (1995). A complex double-couple source mechanism for the Ms 7.2 1929 Grand Banks earthquake. Bulletin of the Seismological Society of America, 85(4), 1003-1020.

Bent, A. L. (1996). Am improved source mechanism for the 1935 Timiskaming, Quebec earthquake from regional waveforms. Pure and Applied Geophysics, 146(1), 5-20. https://doi.org/10.1007/BF00876667

Bent, A. L., Lamontagne, M., Adams, J., Woodgold, C. R., Halchuk, S., Drysdale, J., Wetmiller, R.J., Ma, s., & Dastous, J. B. (2002). The Kipawa, Quebec “Millennium” earthquake. Seismological Research Letters, 73(2), 285-297. https://doi.org/10.1785/gssrl.73.2.285

Bent, A. L., Drysdale, J., & Perry, H. C. (2003). Focal mechanisms for eastern Canadian earthquakes, 1994–2000. Seismological Research Letters, 74(4), 452-468. https://doi.org/10.1785/gssrl.74.4.452

Brooks, G. R., & Adams, J. (2020). A review of evidence of glacially-induced faulting and seismic shaking in eastern Canada. Quaternary Science Reviews, 228, 106070. https://doi.org/10.1016/j.quascirev.2019.106070

Busch, J. P., van der Pluijm, B. A., Hall, C. M., & Essene, E. J. (1996). Listric normal faulting during postorogenic extension revealed by 40Ar/39Ar thermochronology near the Robertson Lake shear zone, Grenville orogen, Canada. Tectonics, 15(2), 387-402. https://doi.org/10.1029/95TC03501

Byerlee, J. (1978), Friction of rocks, Pure Appl. Geophys., 116, 615-626. https://doi.org/10.1007/BF00876528

Calais, E., Camelbeeck, T., Stein, S., Liu, M., & Craig, T. J. (2016). A new paradigm for large earthquakes in stable continental plate interiors. Geophysical Research Letters, 43(20), 10-621. https://doi.org/10.1002/2016GL070815

Collettini, C., & Trippetta, F. (2007). A slip tendency analysis to test mechanical and structural control on aftershock rupture planes. Earth and Planetary Science Letters, 255(3-4), 402-413. https://doi.org/10.1016/j.epsl.2007.01.001

Daneshfar, B., & Benn, K. (2002). Spatial relationships between natural seismicity and faults, southeastern Ontario and north-central New York state. Tectonophysics, 353(1-4), 31-44. https://doi.org/10.1016/S0040-1951(02)00279-2+C12:X13

den Hartog, S. A. M., Faulkner, D. R., & Spiers, C. J. (2020). Low friction coefficient of phyllosilicate fault gouges and the effect of humidity: Insights from a new microphysical model. Journal of Geophysical Research: Solid Earth, 125(6), e2019JB018683. https://doi.org/10.1029/2019JB018683

Doughty, M., Eyles, N., & Eyles, C. (2012). High-resolution seismic reflection profiling of neotectonic faults in Lake Timiskaming, Timiskaming Graben, Ontario-Quebec, Canada. Sedimentology, 60(4), 983-1006. https://doi.org/10.1111/sed.12002

Du, W. X., Kim, W. Y., & Sykes, L. R. (2003). Earthquake source parameters and state of stress for the northeastern United States and southeastern Canada from analysis of regional seismograms. Bulletin of the Seismological Society of America, 93(4), 1633-1648. https://doi.org/10.1785/0120020217

Dupin, J. M., Sassi, W., & Angelier, J. (1993). Homogeneous stress hypothesis and actual fault slip: a distinct element analysis. Journal of Structural Geology, 15(8), 1033-1043. https://doi.org/10.1016/0191-8141(93)90175-A

Dyke, A. S., Andrews, J. T., Clark, P. U., England, J. H., Miller, G. H., Shaw, J., & Veillette, J. J. (2002). The Laurentide and Innuitian ice sheets during the last glacial maximum. Quaternary Science Reviews, 21(1-3), 9-31. https://doi.org/10.1016/S0277-3791(01)00095-6

Hasegawa, H. S., & Kanamori, H. (1987). Source mechanism of the magnitude 7.2 Grand Banks earthquake of November 1929: Double couple or submarine landslide?. Bulletin of the seismological Society of America, 77(6), 1984-2004.

Hasegawa, H. S., Adams, J., & Yamazaki, K. (1985). Upper crustal stresses and vertical stress migration in eastern Canada. Journal of Geophysical Research: Solid Earth, 90(B5), 3637-3648. https://doi.org/10.1029/JB090iB05p03637

Heidbach, O., Tingay, M., Barth, A., Reinecker, J., Kurfeß, D., & Müller, B. (2010). Global crustal stress pattern based on the World Stress Map database release 2008. Tectonophysics, 482(1-4), 3-15. https://doi.org/10.1016/j.tecto.2009.07.023

Horner, R. B., Stevens, A. E., Hasegawa, H. S., & Leblanc, G. (1978). Focal parameters of the July 12, 1975, Maniwaki, Québec, earthquake—An example of intraplate seismicity in eastern Canada. Bulletin of the Seismological Society of America, 68(3), 619-640.

Ito, T., & Zoback, M. D. (2000). Fracture permeability and in situ stress to 7 km depth in the KTB scientific drillhole. Geophysical Research Letters, 27(7), 1045-1048. https://doi.org/10.1029/1999GL011068

Kay, G. M. (1942). Ottawa-Bonnechere graben and Lake Ontario homocline. Bulletin of the Geological Society of America, 53(4), 585-646. https://doi.org/10.1130/GSAB-53-585

Kumarapeli, P. S. (1978). The St. Lawrence paleo-rift system: a comparative study. In Tectonics and Geophysics of Continental Rifts (pp. 367-384). Springer, Dordrecht. https://doi.org/10.1007/978-94-009-9806-3_29

Lamontagne, M., & Ranalli, G. (1996). Thermal and rheological constraints on the earthquake depth distribution in the Charlevoix, Canada, intraplate seismic zone. Tectonophysics, 257(1), 55-69. https://doi.org/10.1016/0040-1951(95)00120-4

Lamontagne, M., Brouillette, P., Grégoire, S., Bédard, M. P., & Bleeker, W (2020). Faults and lineaments of the Western Quebec Seismic Zone, Quebec and Ontario. Geological Survey of Canada, Open File 8361, 28 pp. (1 sheet). https://doi.org/10.4095/321900

Le Pan, N. (2016). Fault Lines: Earthquakes, Insurance, and Systemic Financial Risk. CD Howe Institute Commentary, 454. https://www.cdhowe.org/sites/default/files/attachments/research_papers/mixed/Commentary%20454_0.pdf

Lisle, R. J. (2013). A critical look at the Wallace-Bott hypothesis in fault-slip analysis. Bulletin de la Société Géologique de France, 184(4-5), 299-306. https://doi.org/10.2113/gssgfbull.184.4-5.299

Lisle, R. J., & Srivastava, D. C. (2004). Test of the frictional reactivation theory for faults and validity of fault-slip analysis. Geology, 32(7), 569-572. https://doi.org/10.1130/G20408.1

Lovell, H.L. and Caine, T.W. (1970) Lake Temiskaming Rift Valley. Ontario Department of Mines Miscellaneous Paper 39, 16pp. http://www.geologyontario.mndm.gov.on.ca/mndmfiles/pub/data/records/MP039.html

Ma, S., & Motazedian, D. (2012). Studies on the June 23, 2010 north Ottawa MW 5.2 earthquake and vicinity seismicity. Journal of Seismology, 16(3), 513-534. https://doi.org/10.1007/s10950-012-9294-7

Ma, S., & Audet, P. (2014). The 5.2 magnitude earthquake near Ladysmith, Quebec, 17 May 2013: implications for the seismotectonics of the Ottawa–Bonnechere Graben. Canadian Journal of Earth Sciences, 51(5), 439-451. https://doi.org/10.1139/cjes-2013-0215

Ma, S., & Eaton, D. W. (2007). Western Quebec seismic zone (Canada): Clustered, midcrustal seismicity along a Mesozoic hot spot track. Journal of Geophysical Research: Solid Earth, 112(B6). https://doi.org/10.1029/2006JB004827

Mazzotti, S., & Townend, J. (2010). State of stress in central and eastern North American seismic zones. Lithosphere, 2(2), 76-83. https://doi.org/10.1130/L65.1

McCalpin, J. P. (Ed.) (2009). Paleoseismology, 2nd ed.: International Geophysics Series, Academic Press, 613 p.

Morris, A., Ferrill, D. A., & Henderson, D. B. (1996). Slip-tendency analysis and fault reactivation. Geology, 24(3), 275-278. https://doi.org/10.1130/0091-7613(1996)024<0275:STAAFR>2.3.CO;2

Peace, A. L., Dempsey, E. D., Schiffer, C., Welford, J. K., McCaffrey, K. J., Imber, J., & Phethean, J. J. (2018). Evidence for basement reactivation during the opening of the Labrador Sea from the Makkovik Province, Labrador, Canada: Insights from field data and numerical models. Geosciences, 8(8), 308. https://doi.org/10.3390/geosciences8080308

Pollard, D. D., Saltzer, S. D., & Rubin, A. M. (1993). Stress inversion methods: are they based on faulty assumptions?. Journal of Structural Geology, 15(8), 1045-1054. https://doi.org/10.1016/0191-8141(93)90176-B

Reiter, K., Heidbach, O., Schmitt, D., Haug, K., Ziegler, M., & Moeck, I. (2014). A revised crustal stress orientation database for Canada. Tectonophysics, 636, 111-124. https://doi.org/10.1016/j.tecto.2014.08.006

Richardson, R. M. (1992). Ridge forces, absolute plate motions, and the intraplate stress field. Journal of Geophysical Research: Solid Earth, 97(B8), 11739-11748. https://doi.org/10.1029/91JB00475

Rimando, R. (1994). Tectonic framework and relative ages of structures within the Ottawa–Bonnechère Graben. MSc Thesis, University of Ottawa, Ottawa, Canada.

Rimando, R. E., & Benn, K. (2005). Evolution of faulting and paleo-stress field within the Ottawa graben, Canada. Journal of Geodynamics, 39(4), 337-360. https://doi.org/10.1016/j.jog.2005.01.003

Rimando, J., Schoenbohm, L. M., Ortiz, G., Alvarado, P., Venerdini, A., Owen, L. A., ... & Hammer, S. Late Quaternary intraplate deformation defined by the Las Chacras Fault Zone, West-Central Argentina. Tectonics, e2020TC006509. https://doi.org/10.1029/2020TC006509

Rocher, M., Tremblay, A. (2001). L’effondrement de la plate-forme du Saint-Laurent: ouverture de Iapetus ou de l’Atlantique? Apport dela reconstitution des paléocontraintes dans la régionde Québec (Canada). C. R. Acad. Sci. Paris, Sciences de la Terre et des planets, 333, 171–178. https://doi.org/10.1016/S1251-8050(01)01610-X

Seeber, L., Kim, W. Y., Armbruster, J. G., Du, W. X., Lerner-Lam, A., & Friberg, P. (2002). The 20 April 2002 Mw 5.0 earthquake near Au Sable Forks, Adirondacks, New York: a first glance at a new sequence. Seismological Research Letters, 73(4), 480-489. https://doi.org/10.1785/gssrl.73.4.480

Sibson, R. H. (1989). High-angle reverse faulting in northern New Brunswick, Canada, and its implications for fluid pressure levels. Journal of Structural geology, 11(7), 873-877. https://doi.org/10.1016/0191-8141(89)90104-1

Snee, J. E. L., & Zoback, M. D. (2020). Multiscale variations of the crustal stress field throughout North America. Nature communications, 11(1), 1-9. https://doi.org/10.1038/s41467-020-15841-5

Stein, S. (2007). Approaches to continental intraplate earthquake issues, in Continental intraplate earthquakes: Science, hazard, and Policy Issue. Geological Society of American Spectrum Paper, 425, 1–16. https://doi.org/10.1130/2007.2425(01)

Townend, J., & Zoback, M. D. (2000). How faulting keeps the crust strong. Geology, 28(5), 399-402. https://doi.org/10.1130/0091-7613(2000)28<399:HFKTCS>2.0.CO;2

Tuttle, M. P., Schweig, E. S., Sims, J. D., Lafferty, R. H., Wolf, L. W., & Haynes, M. L. (2002). The earthquake potential of the New Madrid seismic zone. Bulletin of the Seismological Society of America, 92(6), 2080-2089. https://doi.org/10.1785/0120010227

Wahlström, R. (1987). Focal mechanisms of earthquakes in southern Quebec, southeastern Ontario, and northeastern New York with implications for regional seismotectonics and stress field characteristics. Bulletin of the Seismological Society of America, 77(3), 891-924.

Wallach, J., Benn, K., & Rimando, R. (1995). Recent, tectonically induced, surficial stress-relief structures in the Ottawa–Hull area, Canada. Canadian Journal of Earth Sciences, 32(3), 325-333. https://doi.org/10.1139/e95-027

Wallach, J., & Chagnon, J. Y. (1990). The occurrence of pop-ups in the Québec City area. Canadian Journal of Earth Sciences, 27(5), 698-701. https://doi.org/10.1139/e90-068

Wallach. J.L., Mohajer, A.A., McFall, G.H., Bowlby, J.R., Pearce, M. and McKay, D.A. (1993). Pop-ups as geological indicators of earthquake-prone areas in intraplate eastern North America. In L.A. Owen, I. Stewart, and C. Vita-Finzi, eds., Neotectonics: Recent Advances. Quaternary Proceedings, 3, 67-83.

Worum, G., van Wees, J. D., Bada, G., van Balen, R. T., Cloetingh, S., & Pagnier, H. (2004). Slip tendency analysis as a tool to constrain fault reactivation: A numerical approach applied to three-dimensional fault models in the Roer Valley rift system (southeast Netherlands). Journal of Geophysical Research: Solid Earth, 109(B2). https://doi.org/10.1029/2003JB002586

Zoback, M. L. (1992). Stress field constraints on intraplate seismicity in eastern North America. Journal of Geophysical Research: Solid Earth, 97(B8), 11761-11782. https://doi.org/10.1029/92JB00221

Zoback, M. D., & Townend, J. (2001). Implications of hydrostatic pore pressures and high crustal strength for the deformation of intraplate lithosphere. Tectonophysics, 336(1-4), 19-30. https://doi.org/10.1016/S0040-1951(01)00091-9

Zoback, M. D., and M. L. Zoback (2002), State of stress in the Earth's lithosphere, in International Handbook of Earthquake and Engineering Seismology, Int. Geophys. Ser., edited by W. H. K. Lee, P. C. Jennings, and H. Kanamori, pp. 559–568, Academic Press, Amsterdam.